NACA RM E57F03

NACA

RESEARCH MEMORANDUM

EFFECTS OF INTERNAL-AREA DISTRIBUTION, SPIKE TRANSLATION, AND THROAT BOUNDARY-LAYER CONTROL ON PERFORMANCE OF A DOUBLE-CONE AXISYMMETRIC INLET AT MACH NUMBERS FROM 3.0 TO 2.0

By James F. Connors, J. Calvin Lovell, and George A. Wise

Lewis Flight Propulsion Laboratory
Cleveland, Ohio

NATIONAL ADVISORY COMMITTEE
FOR AERONAUTICS
WASHINGTON

August 30, 1957
Declassified December 8, 1961

1Z

NACA RM E57F03

NATIONAL ADVISORY COMMITTEE FOR AERONAUTICS

RESEARCH MEMORANDUM

EFFECTS OF INTERNAL-AREA DISTRIBUTION, SPIKE TRANSLATION, AND THROAT BOUNDARY-LAYER CONTROL ON PERFORMANCE OF A DOUBLE-CONE AXISYMMETRIC INLET AT MACH NUMBERS FROM 3.0 TO 2.0

4541

By James F. Connors, J. Calvin Lovell, and George A. Wise

SUMMARY

An investigation was made to determine the effects of initial subsonic diffusion rate, variable geometry, and throat boundary-layer control on the performance of an axisymmetric double-cone inlet. Results were obtained for Mach numbers from 3.0 to 2.0, angles of attack to 12°, and a Reynolds number of 3.07×10^{6} based on the capture diameter.

Major gains in performance at the higher Mach numbers were obtained with boundary-layer control in the form of a ram scoop at the throat. Compared with the no-bleed configuration at Mach 3.01, the total-pressure recovery was increased from 0.625 to 0.74, with a concomitant increase in the cowl-plus-spillage drag coefficient from 0.11 to 0.14 due to a corresponding decrease in the mass-flow ratio from 0.96 to 0.91. This resulted in an improvement of 22 percent in propulsive thrust for a hypothetical turbojet engine with such a bleed system. Below Mach 2.1 where shock detachment occurred, boundary-layer bleed was not effective.

Minor improvements in internal performance were obtained at the higher Mach numbers (above 2.44) with a more gradual area expansion in the initial portion of the subsonic diffuser. However, as the spike was retracted, internal contraction was also encountered sooner. At reduced Mach numbers, fixed-geometry configurations incurred excessively high-spillage drags and somewhat lower pressure recoveries when compared with those of a translating-spike inlet.

INTRODUCTION

The first phase of an extensive program on axisymmetric double-cone inlets, designed for operation over a range of Mach numbers up to 3.0, has been reported in reference 1. It was found that an inlet with a

rapid turn on the spike shoulder (the 20-percent-cowl inlet) gave essentially the same internal performance with 45 percent less cowl drag than an inlet with a more gradual turn (the 40-percent-cowl inlet). These results indicated an obvious preference for the lower drag configuration in terms of over-all performance.

With the 20-percent-cowl inlet of reference 1 used as a figure of comparison, the present investigation evaluated in detail the effects on performance of several design variables. Specifically, these design variations included the use of a more gradual initial rate of area expansion in the subsonic duct, a comparison of a fixed-geometry inlet with a translating-spike configuration, and the application of various boundary-layer control techniques. Boundary-layer bleed systems using either ram scoops or flush slots in the vicinity of the throat were explored. Pumping of the bleed air was accomplished by venting the centerbody and aspirating to ambient pressure. These modifications were evaluated on the basis of a net propulsive thrust in order to indicate the balance between internal performance and external drag.

Generally, spike translation was programmed on the basis of matching the airflow requirements of a hypothetical turbojet engine by spilling air with the first oblique shock and, where possible, keeping the second oblique positioned at the cowl lip. At design Mach number (3.0), both oblique shocks coalesced at the cowl lip.

The investigation was conducted in the Lewis 10- by 10-foot unitary wind tunnel at Mach numbers of 3.01, 2.73, 2.44, and 1.97. Reynolds number based on the inlet capture diameter was constant at 3.07×10^6, and angle of attack was varied up to 12°.

SYMBOLS

A	area, sq ft
A_{in}	inlet capture area, 1.184 sq ft
A_{max}	maximum projected frontal area of model, 1.483 sq ft
A_x	area normal to flow direction in duct, sq in.
A_3	diffuser-exit flow area, 0.961 sq ft
C_D	drag coefficient, $D/q_0 A_{max}$
D	drag, lb

4541

D_a additive drag

D_c cowl drag

D_{c+s} cowl pressure drag plus spillage (additive plus bleed) drag

F thrust, lb

F_{id} ideal thrust, i.e., F at $\overline{P}_3/P_0 = 1.0$, lb

M Mach number

m_3/m_0 inlet mass-flow ratio, $\rho_3 V_3 A_3/\rho_0 V_0 A_{in}$

P total pressure, lb/sq ft

$\overline{P}_3/P_0$ total-pressure recovery

q dynamic pressure, lb/sq ft

V air velocity, ft/sec

w weight flow, lb/sec

$\frac{w\sqrt{\theta}}{\delta A_3}$ corrected weight flow at station 3, (lb/sec)/sq ft

x distance along axis of symmetry, in.

Y distance across the duct normal to the average duct flow, in.

y distance from axis of symmetry or distance from centerbody normal to the average duct flow, in.

α angle of attack, deg

δ ratio of local total pressure to NACA standard sea-level pressure of 2116, lb/sq ft

η propulsive-thrust parameter, $\frac{F - D_{c+s}}{F_{id}}$

θ ratio of local total temperature to NACA standard sea-level temperature of 518.7° R

θ_l cowl-position parameter, angle between axis of symmetry and line from spike tip to cowl lip, deg

ρ density of air, lb/cu ft

Subscripts:

max maximum

0 conditions in free stream

3 conditions at diffuser exit

Superscript:

$\bar{}$ area-weighted value

APPARATUS AND PROCEDURE

A schematic drawing of the over-all inlet test model is shown in figure 1(a). This is the 20-percent-cowl inlet model with a maximum diameter of 16.46 inches that was used in reference 1. Briefly, the model incorporated a movable exit plug to vary the back pressure, an internal balance, and provisions for translating the spike and varying the angle of attack. The basic supersonic-compression surface consisted of a 20°-35° double-cone centerbody designed for both oblique shocks to coalesce at the cowl lip at Mach 3.0.

Modifications for the application of boundary-layer control are indicated in figure 1(b). The drawing of the inlet test model shows how the centerbody was vented to ambient pressure through two hollow support struts. Small semicones were attached to the external skin over the struts for better pumping of the bleed air through ejector action. Figure 1(b) also shows sketches of the various bleed configurations studied. Ram scoops (1 and 2) and the flush slot are drawn to scale with the cowl lip in the design position (M = 3.0). As an additional point of reference, the inlet station is represented by a line from the cowl lip perpendicular to the second conical surface. The height of ram scoop 2 was approximately one boundary-layer thickness.

To contrast with the inlet of reference 1, which will be hereinafter referred to as inlet I, another configuration designated as inlet II was designed for the same cowl but with a different internal-area distribution (see fig. 1(c)). At Mach 3.01, inlet II had a more gradual initial rate of area expansion in the subsonic duct (an equivalent conical area expansion of approximately 18.5°, compared with 42° for inlet I). Inlet II characteristically incurred internal contraction earlier with spike retraction; for example, at the Mach 2.44 positions, inlet II already had internal contraction and inlet I did not. Coordinate dimensions are given in tables I and II.

Instrumentation and data-reduction methods were the same as those employed in reference 1. For convenience, the principal parameters and their method of determination are tabulated as follows:

Parameter	Basis of calculation
Total-pressure recovery, $\bar{P}_3/P_0$	Area-weighted average of 48 total pressures at station 66
Mass-flow ratio, m_3/m_0	Static pressure at station 66 and the assumption of isentropic flow to choked area at plug
External drag, D	Difference between axial force obtained from balance and internal thrust calculated from pressures
Cowl drag, D_c	Integration of experimental static-pressure distributions
Additive drag, D_a	Subtraction of the measured cowl drag and an estimated friction drag from the total external drag (for the no-bleed configurations)

Additional total-pressure rakes were installed inside the annular duct at stations 0 and 16 for local flow surveys to determine the approximate location of high-loss areas.

RESULTS AND DISCUSSION

This section will be subdivided into three main areas of investigation. (1) With the basic double-cone inlet of reference 1 used for comparison, the effects of a more gradual internal-area distribution at the beginning of the subsonic diffuser are illustrated. (2) The performance gains due to variable geometry are shown in a comparison of fixed-geometry and translating-spike configurations. (3) The last and most significant subdivision is a discussion of the major performance gains resulting from the application of boundary-layer control in the vicinity of the throat. Performance of the various configurations is described in terms of total-pressure recovery, mass-flow rate, and external-drag coefficients.

Effect of Internal-Area Distribution

The individual performance curves for inlet II at design values of cowl-position parameter θ_1 are presented in figure 2, for Mach numbers

of 3.01, 2.73, and 2.44. At Mach 3.01, inlet II which had the more gradual rate of area expansion attained a pressure recovery of 0.645, as compared with 0.625 for inlet I. Additional performance curves for values of θ_l greater than design and at the free-stream Mach number M_0 of 3.01 are shown in figure 3(a). The effect of θ_l on performance at Mach 3.01 was markedly different for the two inlets (see fig. 3(b)). With inlet II, increasing θ_l 1/2 degree above the design value gave a stable subcritical operating range $\Delta m_3/m_0$ of approximately 0.4. This stability, however, was accompanied by a 0.04 decrease in maximum recovery. These results are in contrast to the results obtained with inlet I, but similar to those obtained with the 40-percent-cowl inlet of reference 1. It appears, then, that the rapid area expansion of inlet I, rather than the rapid rate of turning, triggered subcritical-flow instability (or buzz). Presumably, the rapid area expansion induced flow separation and choking within the duct to initiate the buzz condition.

4541

The variation of critical performance for both inlets I and II at design θ_l with free-stream Mach number is shown in figure 4. Inlet II resulted in a slight improvement in pressure recovery (0.01 to 0.02) above that for inlet I at each Mach number investigated. Mass-flow ratios at Mach 2.44 and above were about the same for both configurations. As Mach number is decreased below 2.44, shock detachment and an attendant decrease in mass-flow ratio due to excessive internal contraction would occur at a somewhat higher Mach number for inlet II than for inlet I. This is indicated qualitatively on the figure by the droop in the mass-flow curve for inlet II.

Effect of Spike Translation

Critical inlet performance of the fixed-geometry configuration is also included in figure 4 for Mach numbers from 3.0 to 2.0. Pressure recoveries for the fixed inlet were several counts lower than those for the translating-spike inlets at the intermediate Mach numbers. Presumably, the higher recoveries of the variable-geometry inlets resulted from the initial rate of area expansion in the subsonic duct being reduced by translation of the spike for reduced Mach-number operation. As Mach number was reduced from the design value (3.0), mass-flow ratio decreased linearly and much more rapidly with the fixed spike. The schedule of pressure recovery and mass flow for the fixed-geometry inlet corresponded to an approximately constant corrected-airflow rate over the Mach-number range studied.

External drag coefficients for supercritical inlet operation are presented in figure 5. Compared with the values for the two translating-spike configurations, the drag coefficients for the fixed-geometry inlet

were much higher at reduced Mach numbers (as much as 50 percent higher at Mach numbers 2.2 to 2.5). This, of course, was a consequence of the increased mass-flow spillage associated with the fixed spike.

Figure 6 shows schlieren photographs of the airflow patterns at zero angle of attack. For the variable-geometry case, the spike was translated to maintain the second oblique shock at the cowl lip. With the fixed spike, both oblique shocks steepened and moved progressively out ahead of the cowl as Mach number was reduced. At $M_0 = 1.97$, both inlets were operating with subsonic entrance flow as indicated by the bow shock standing out ahead of the cowl lip.

4541

Effect of Throat Boundary-Layer Control

Surveys of the flow along the duct of inlet II with no bleed were made at Mach 3.01 primarily to ascertain the distribution and location of total-pressure losses in the inlet. Total-pressure profiles were obtained for zero-angle-of-attack operation at station 0 (at the cowl lip before turning), at station 16 (after the turning back to axial had been completed), and at station 66 (the diffuser exit). Results are shown in figure 7. With supercritical inlet operation (fig. 7(a)), the rake at station 0 indicated essentially a theoretical shock-loss recovery of approximately 0.74. At about the critical condition (fig. 7(b)), the rake at station 16 indicated a local recovery of not more than 0.01 higher than the over-all recovery of 0.645. Thus, the region where the large losses in recovery occurred (0.74 to 0.65) was between stations 0 and 16, where the flow turning was taking place. This is the area where improvements in performance would seem to be most probable with adequate boundary-layer control.

During subcritical inlet operation (fig. 7(c)), a large increase in recovery was observed at the diffuser entrance (station 0). Locally, the recovery at this station was as high as 0.86 at $M_0 = 3.01$. This gain was not realized at the downstream stations. From the inlet total-pressure profile, it was possible to construct a model of the corresponding flow field. The analysis indicated that the additional compression was the result of a third oblique shock generated by a boundary-layer separation wedge caused by pressure feedback from the terminal shock system. The effective aerodynamic wedge was calculated to be approximately 13°.

Diffuser performance characteristics are presented in figure 8 for inlet I with ram scoop 2 located in the vicinity of the throat. Of the various bleed systems investigated, this configuration gave the best over-all performance. At Mach 3.01, a critical recovery of 0.74 was obtained at zero angle of attack with a corresponding mass-flow ratio of 0.91 and

a cowl-position parameter of 29.3°. In most cases with bleed, it was necessary to make slight adjustments in θ_l from the design value. With ram scoop 2 at Mach 3.01, for example, θ_l was 0.2° less than the design value. At design θ_l, the large gains in recovery were not realized. This probably indicates the sensitivity of bleed location relative to the terminal shock.

Critical inlet performances for the various bleed systems are summarized and compared with the no-bleed results of reference 1 in figure 9. In general, all bleed configurations improved recovery. At Mach 3.01, a maximum recovery of 0.765 was achieved with ram scoop 1, but at the expense of a 0.125 decrease in mass-flow ratio and detached-shock operation at $M_0 = 2.73$, caused by the rather blunt scoop and effective internal contraction. Compared with the no-bleed data of reference 1, ram scoop 2 gave large gains in performance at $M_0 = 3.01$ (recovery increased from 0.625 to 0.74 with corresponding mass-flow ratios of 0.96 and 0.91). The recovery gains diminished as Mach number was reduced to 1.97 and were accompanied by a 0.04 to 0.05 decrease in mass-flow ratio from the no-bleed values over the entire Mach-number range. This additional spillage occurred partly behind the shock system at the lip and partly through the internal bleed system. As shown on figure 9, some improvement occurred with the flush-slot configuration, but not as much as with the ram scoops.

Flow surveys along the duct at zero angle of attack were also made with the optimum bleed configuration (inlet I with ram scoop 2) at Mach 3.01. Results are shown in figure 10. In all cases during supercritical inlet operation (fig. 10(b)), the entrance rake at station 0 indicated shock-loss recovery near the cowl lip and slightly increasing recovery towards the centerbody. This shows, possibly, that the ram scoop was not taking the boundary-layer flow off cleanly and actually was forcing some separation in front of it to generate additional compression. At approximately critical operation (fig. 10(a)), all three rakes were close to the same recovery levels. From this it is concluded that the subsonic duct losses were reasonably small, and the terminal shock system was located near the design position or minimum area station during critical operation. It appears that the ram scoop allowed the inlet to benefit from the added compression due to separation and removed enough of the low-energy air to prevent breakdown of the flow into the subsonic duct (e.g., separation). This type of flow mechanism had been previously observed and described at lower Mach numbers with two-dimensional inlets (see ref. 2).

The effect of angle of attack on inlet performance with and without boundary-layer control is presented in figure 11. The pressure recovery with bleed (ram scoop 2) dropped off more rapidly with angle of attack

4541

than with no bleed. This decrease appears generally typical of high-recovery inlets. At Mach 3.01 and an angle of attack of 10°, both inlets had about the same recovery. Mass-flow ratios with bleed were lower at $\alpha = 0$ than the no-bleed values, but the rate of drop off in mass flow was about the same for both cases.

Variation of mass-flow ratio and pressure recovery with the cowl-position parameter θ_l is shown in figure 12. By comparing the bleed data with that for the no-bleed case at corresponding values of θ_l, the mass-flow ratio through the internal bleed system may be determined, and also the amount of shock spillage. For example, at Mach 3.01 with bleed, the capture mass-flow ratio was 0.91, bleed mass-flow ratio was 0.025, and the shock spillage mass-flow ratio was 0.065. Bleed mass-flow ratio remains essentially constant (~0.02) down to Mach 2.44, but increased to 0.05 at $M_0 = 1.97$, probably as a result of detached-shock operation.

4541

In figure 13, a propulsive-thrust comparison was made of inlet I without and with boundary-layer control in the form of ram scoop 2. The upper portion of the figure presents the cowl-plus-spillage drag coefficients for both cases over the Mach-number range. With bleed, these coefficients are 0.01 to 0.03 higher than the no-bleed values. At Mach 3.01, the cowl-plus-spillage drag coefficient (based on the maximum frontal area) was 0.14 with bleed and 0.11 without bleed. This increased drag with bleed was, of course, the result of the added shock spillage and the dumping of the internal bleed flow through an axial sonic discharge to ambient pressure. These drag coefficients were used in the computations of the propulsive-thrust parameter η (shown in the lower portion of fig. 13). With the inlets matched at the critical condition for all Mach numbers, a turbojet engine with afterburning to 3500° R was assumed in the comparison. With these inlets at the design Mach number, 61.5 percent of ideal thrust would be available with bleed, as compared with about 50.5 percent without bleed. Thus, at Mach 3.01, this system of throat bleed produced an increase in propulsive thrust of 22 percent above the no-bleed value. The shaded portion of this figure shows the gains available with bleed over the Mach-number range. These gains which decrease with Mach number are zero at $M_0 = 2.1$, below which shock detachment occurred, and the slight improvement in recovery was more than offset by the increased drag.

SUMMARY OF RESULTS

An experimental study was made in the 10- by 10-foot supersonic wind tunnel of the performance of an axisymmetric double-cone inlet to determine (1) the effects of variation in the rate of internal area expansion in the initial portion of the subsonic diffuser, (2) the effectiveness of centerbody translation as opposed to a fixed-geometry inlet configuration, and (3) the effect of boundary-layer control in the vicinity of the throat. The following results were obtained:

1. Major gains in performance at the higher Mach numbers were obtained with boundary-layer control in the form of a ram scoop at the throat. At a free-stream Mach number of 3.01, bleed increased the recovery from 0.625 to 0.74 with a corresponding increase in cowl-plus-spillage drag coefficient from 0.11 to 0.14, as mass-flow ratio decreased from 0.96 to 0.91. This corresponds to a 22 percent increase in propulsive thrust for a hypothetical turbojet engine. Below the free-stream Mach number of 2.1, where shock detachment occurred, boundary-layer bleed lost its effectiveness.

2. In comparison with an inlet having a rapid rate of turning and a rapid initial rate of area expansion, minor improvements in internal performance were obtained at Mach numbers from 3.01 to 2.44 by employing a more gradual initial rate of area expansion in the subsonic diffuser (0.645 recovery at Mach 3.01); however, internal contraction was also encountered sooner as the spike was retracted for reduced Mach-number operation. At a free-stream Mach number of 3.01, a large stable subcritical range, equal to 40 percent of maximum mass flow, was obtained by increasing the cowl-position parameter 1/2 degree above design.

3. At reduced Mach numbers, fixed-geometry configurations incurred excessively high-spillage drags (in some cases, as much as 50 percent higher) and somewhat lower pressure recoveries when compared with those of a translating-spike inlet.

Lewis Flight Propulsion Laboratory
National Advisory Committee for Aeronautics
Cleveland, Ohio, June 13, 1957

4541

REFERENCES

1. Connors, James F., Wise, George A., and Lovell, J. Calvin: Investigation of Translating-Double-Cone Axisymmetric Inlets with Cowl Projected Areas 40 and 20 Percent of Maximum at Mach Numbers from 3.0 to 2.0. NACA RM E57C06, 1957.

2. Obery, Leonard J., and Schueller, Carl F.: Effects of Internal Boundary-Layer Control on the Performance of Supersonic Aft Inlets. NACA RM E55L17, 1956.

4541

TABLE I. - SPIKE COORDINATES

(a) Inlet I.

x, in.	y, in.	
0	0	Straight 20°
10.50	3.82	
11.30	4.376	Straight 35°
13.65	6.027	
13.91	6.165	
14.21	6.220	
14.71	6.246	
15.71	6.280	
16.81	6.300	
18.41	6.265	
19.71	6.228	
21.21	6.190	
22.71	6.150	
24.71	6.105	
26.21	6.060	

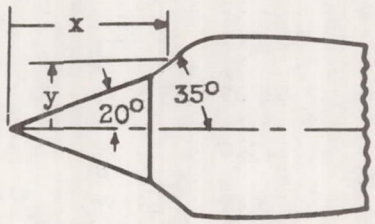

(b) Inlet II.

x, in.	y, in.	
0	0	Straight 20°
10.50	3.82	
11.30	4.376	Straight 35°
11.71	4.669	
13.86	6.174	
14.11	6.320	
14.41	6.407	
14.71	6.452	
15.01	6.472	
15.31	6.480	
16.51	6.480	
18.41	6.440	
19.71	6.405	
23.71	6.255	
25.21	6.170	
26.21	6.060	

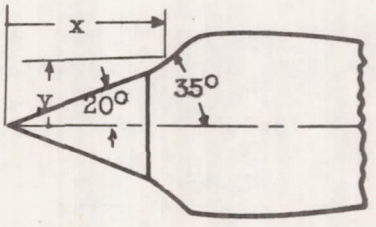

4541

TABLE II. - COWL COORDINATES

Station	Diameter, in.	
	Internal	External
0.01	14.730	14.770
.50	------	15.384
.60	15.344	------
.80	15.514	15.690
1.10	15.700	15.896
1.40	15.840	16.052
1.80	15.964	16.184
2.20	16.044	16.270
2.60	16.100	16.310
3.00	16.140	16.350
3.50	16.174	16.384
4.50	16.190	16.400
5.00	16.200	16.436
6.00	16.210	16.460
7.00	16.200	
8.00	16.180	
9.00	16.160	
10.00	16.150	
11.00	16.130	
12.00	16.110	
13.00	16.064	
14.00	16.024	
15.00	15.984	
16.00	15.944	
17.00	15.904	
18.00	15.864	
19.00	15.820	
20.00	15.780	
21.00	15.740	
22.00	15.700	
22.50	15.680	

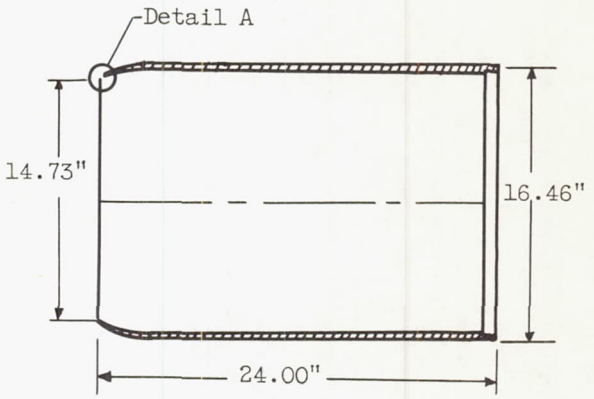

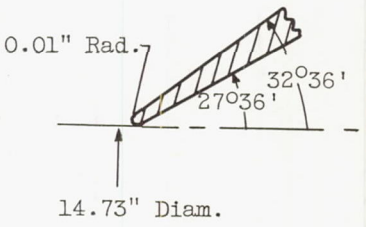

Detail A

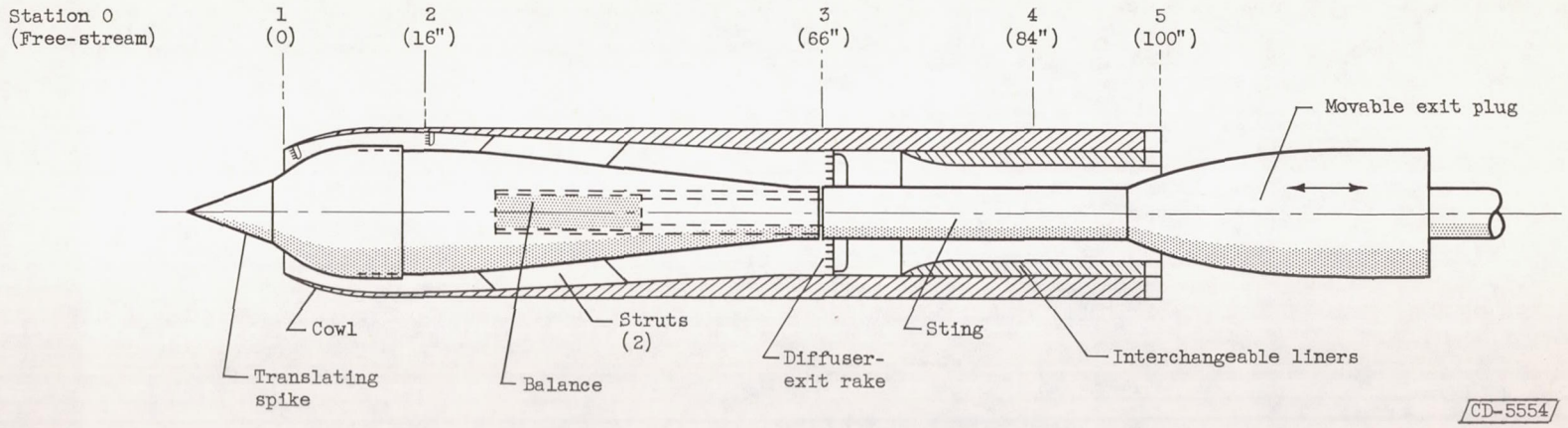

(a) Schematic drawing of inlet test model.

Figure 1. - Experimental apparatus.

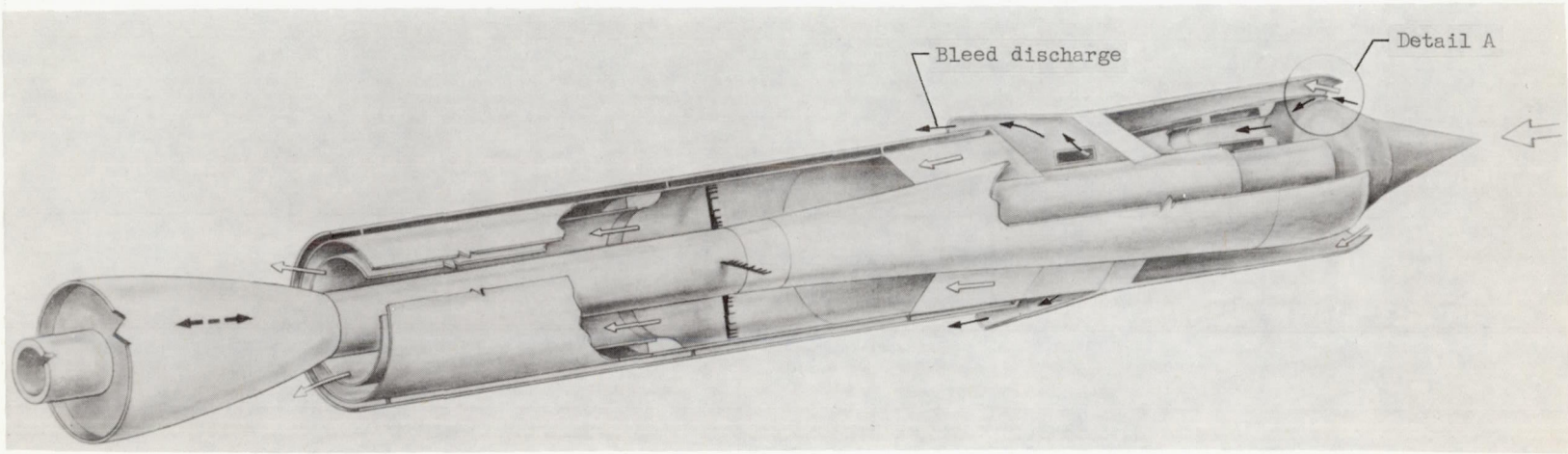

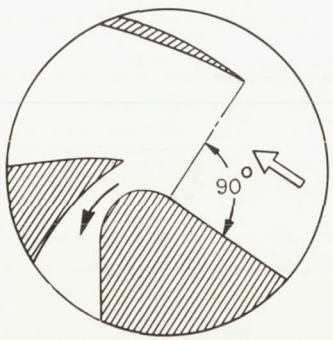

Ram scoop 1

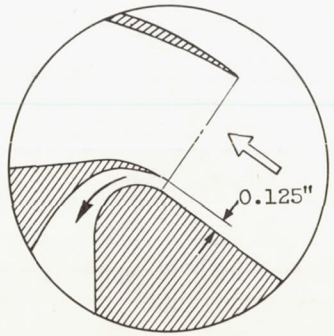

Ram scoop 2

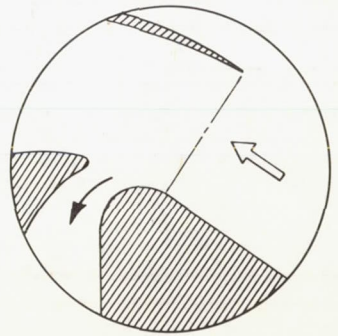

Flush slot

CD-5643

Detail A (θ_l = 29.5°)

(b) Boundary-layer bleed systems.

Figure 1. - Continued. Experimental apparatus.

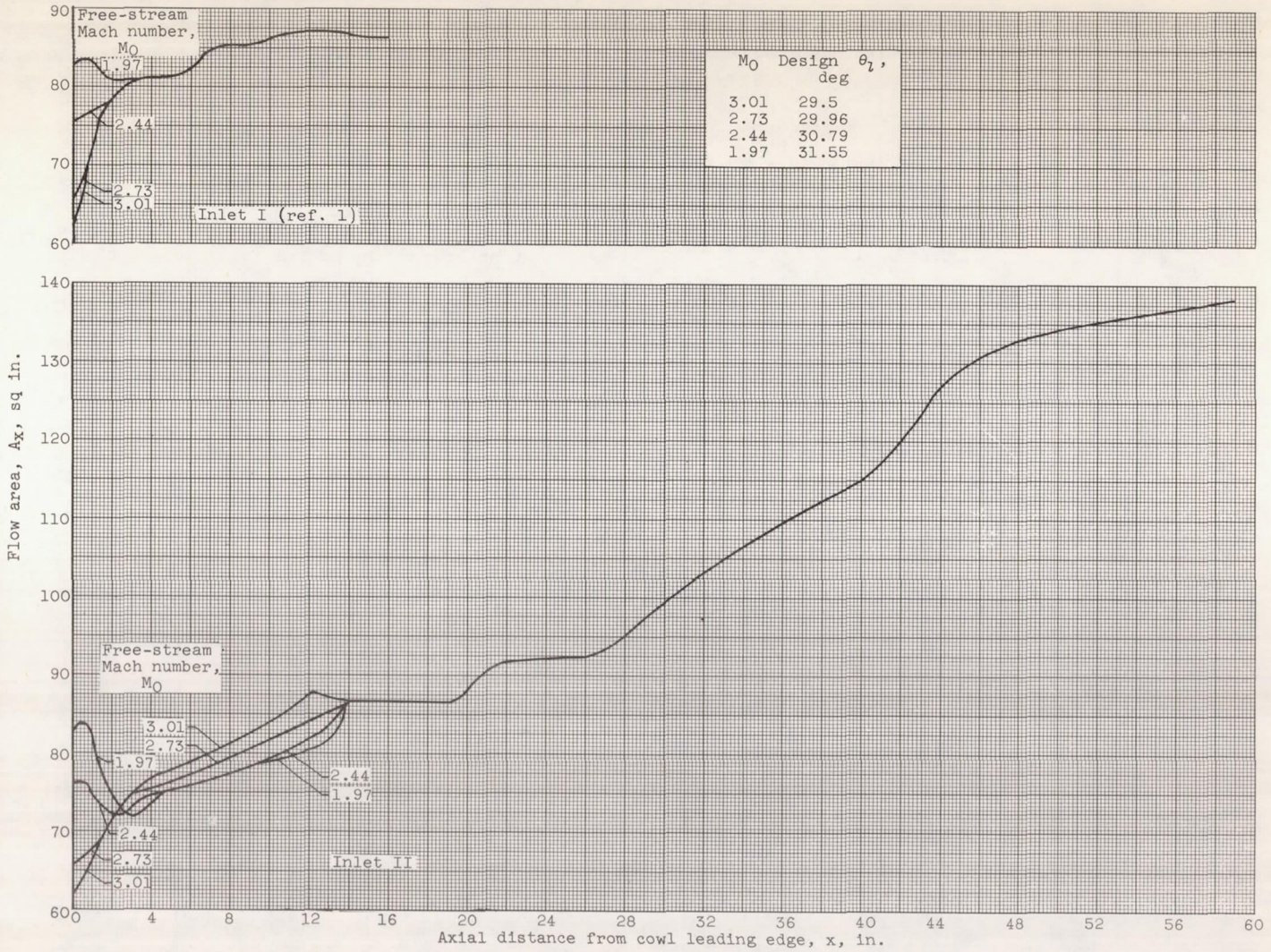

(c) Internal-area distribution.

Figure 1. - Concluded. Experimental apparatus.

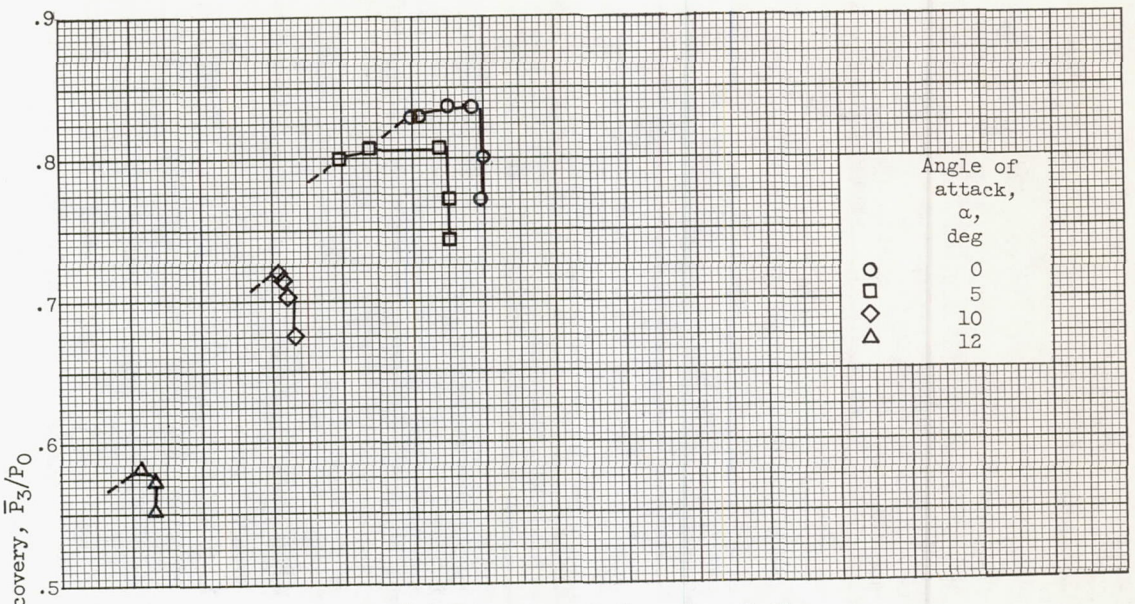

(a) Free-stream Mach number, 2.44.

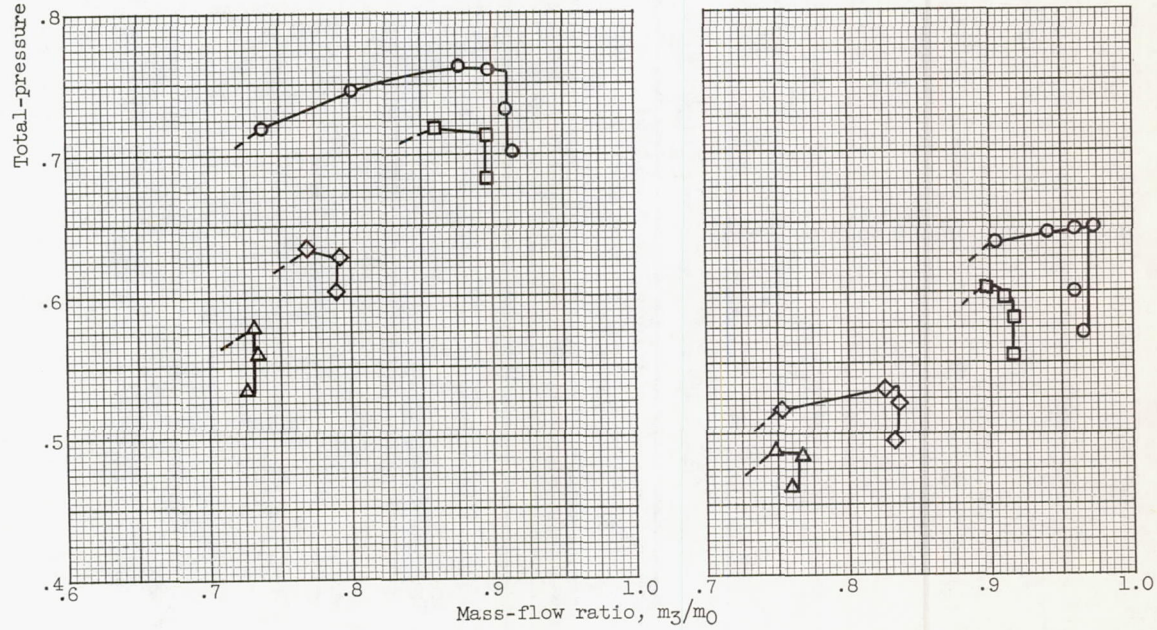

(b) Free-stream Mach number, 2.73.

(c) Free-stream Mach number, 3.01.

Figure 2. - Diffuser performance characteristics at design θ_l for each Mach number. Translating spike, inlet II.

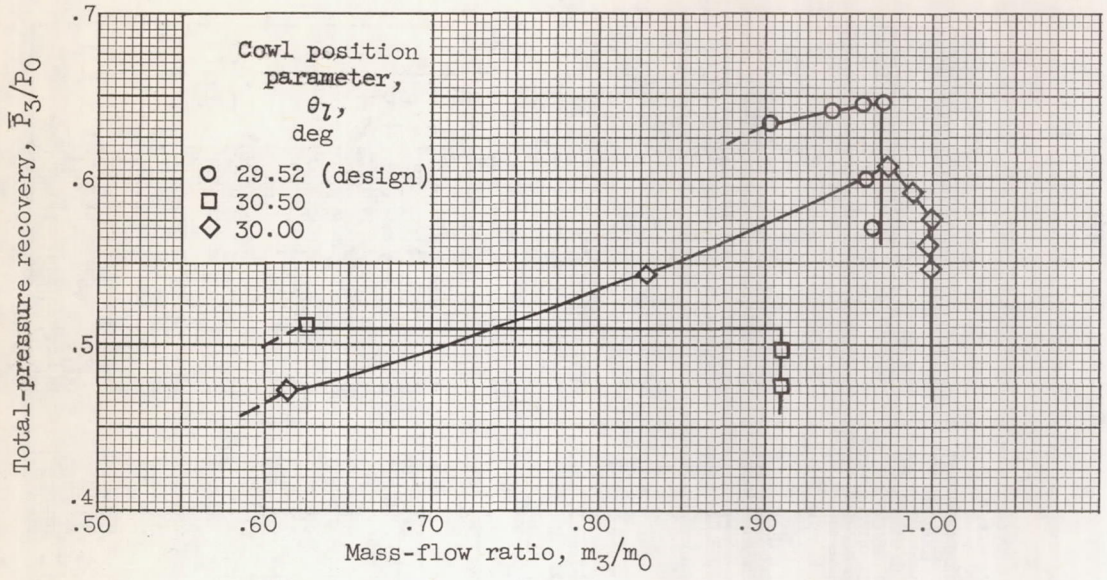

(a) Diffuser characteristics, inlet II.

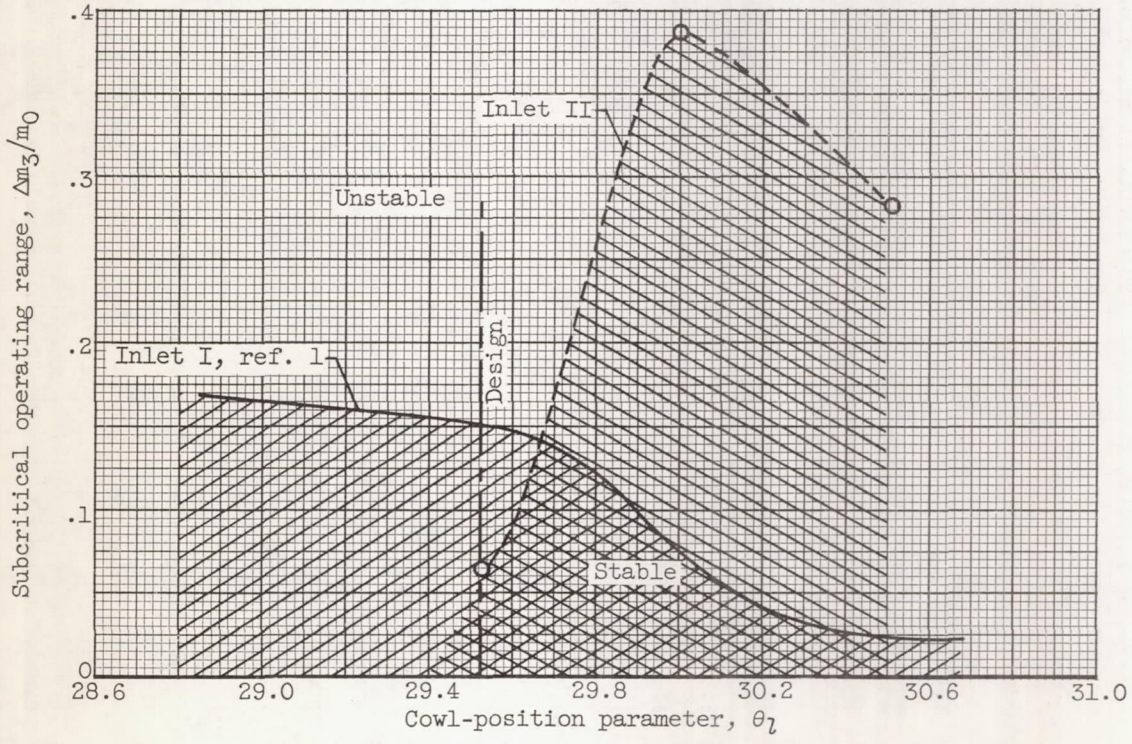

(b) Subcritical stability range.

Figure 3. - Effect of spike translation on inlet performance. Free-stream Mach number, 3.01.

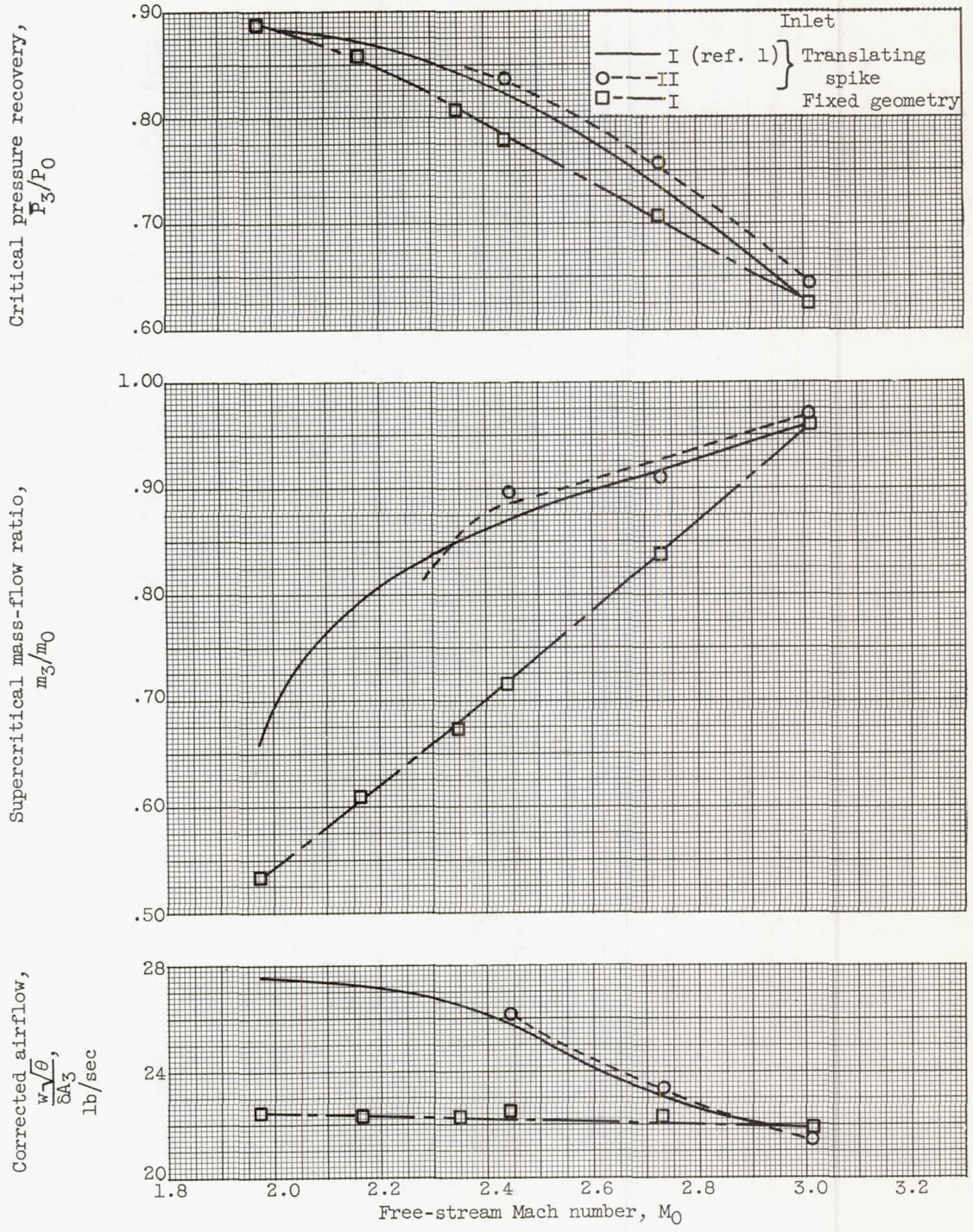

Figure 4. - Variation of critical inlet performance with free-stream Mach number.

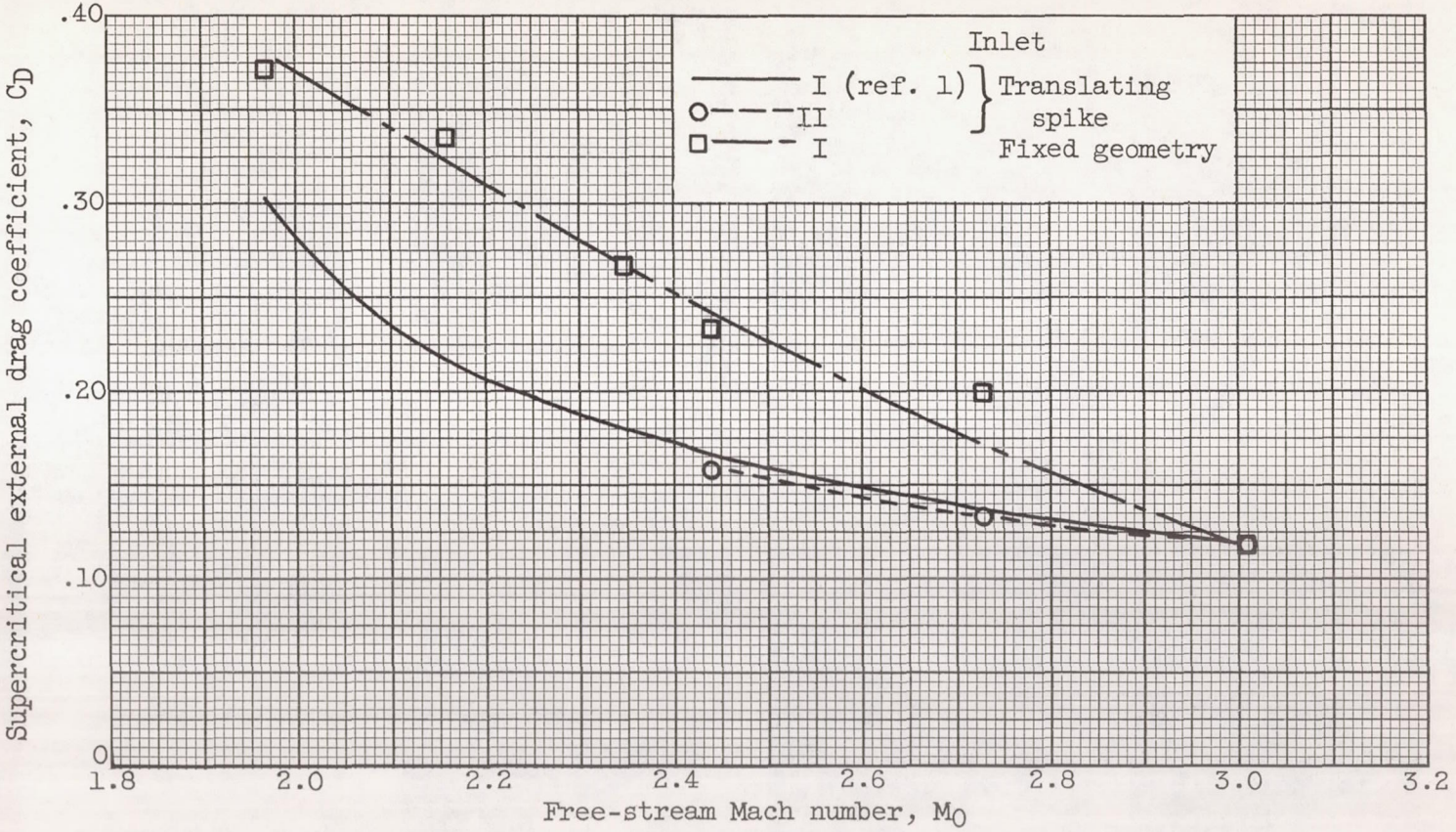

Figure 5. - Variation of supercritical drag coefficients with Mach number for the no-bleed configurations.

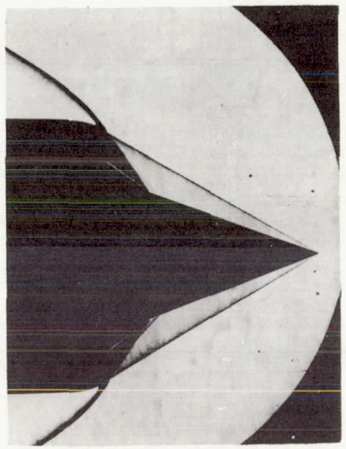

M_0 = 3.01

(a) Design Mach number (same for both inlets).

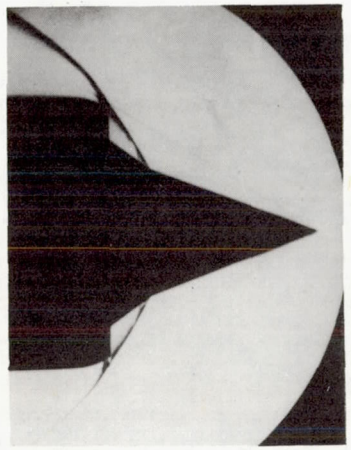

M_0 = 2.73

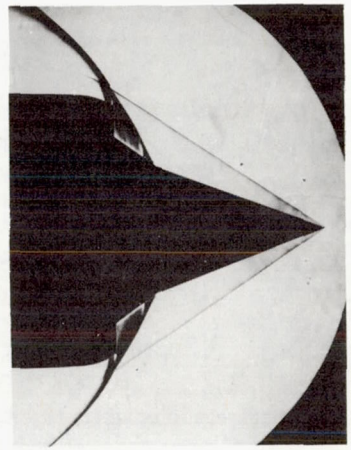

M_0 = 2.44

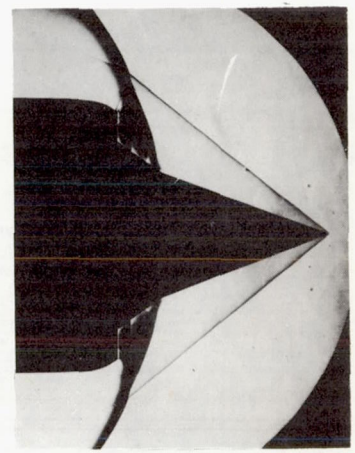

M_0 = 1.97

(b) Fixed-geometry inlet.

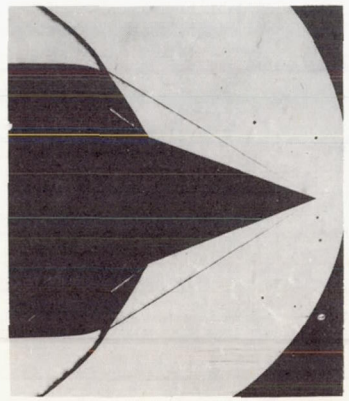

M_0 = 2.73

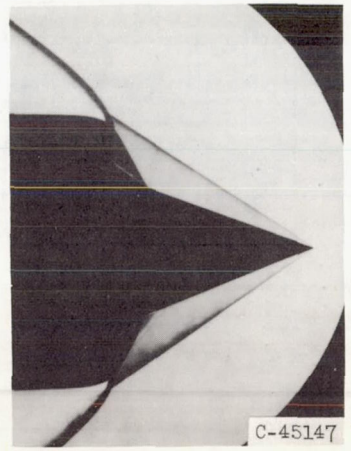

M_0 = 2.44

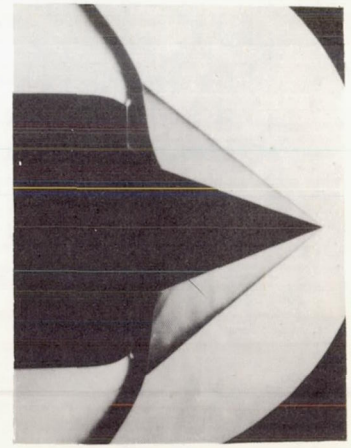

M_0 = 1.97

(c) Translating-spike inlet.

Figure 6. - Airflow pattern at zero angle of attack for fixed-geometry and translating-spike inlets.

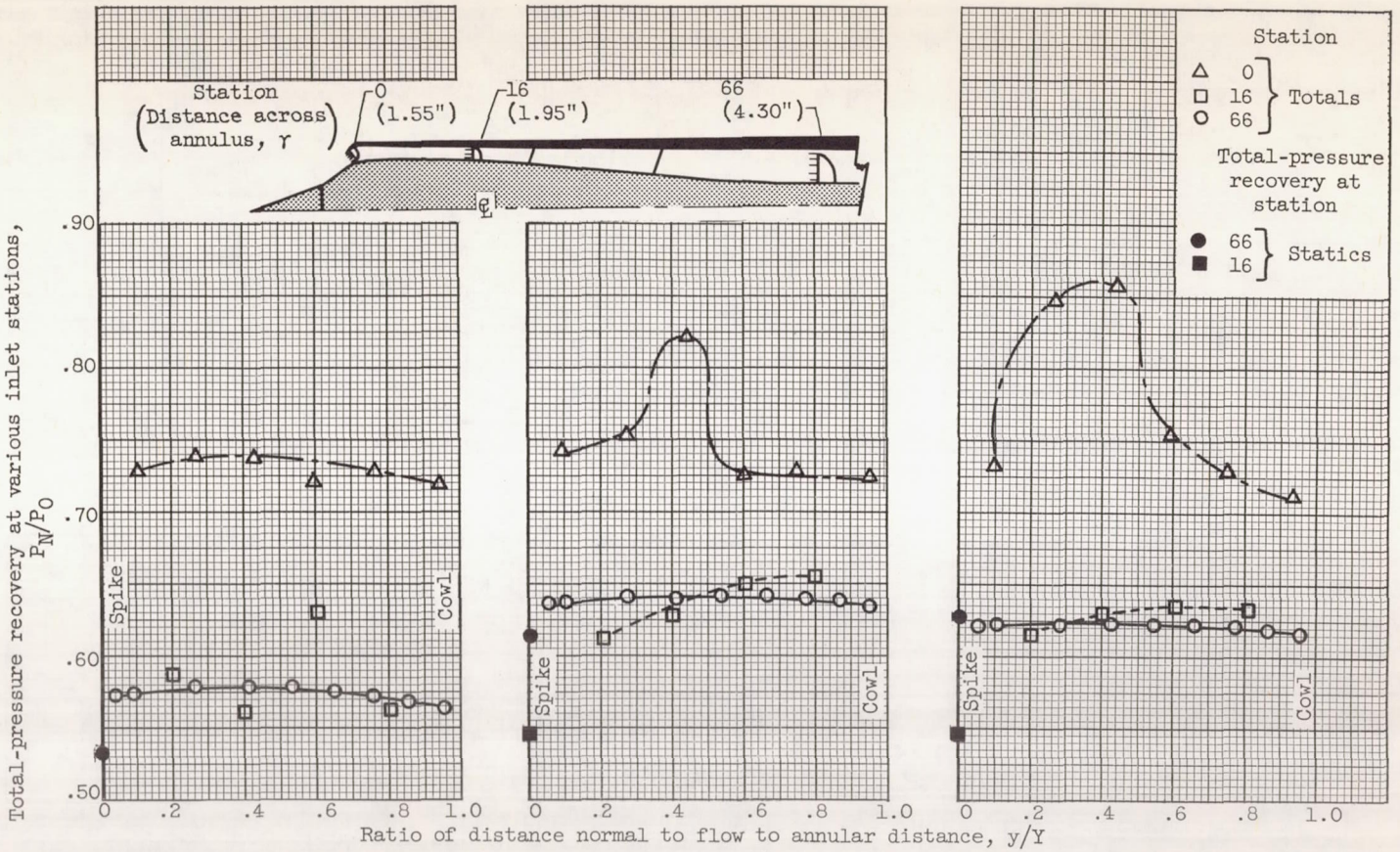

(a) Total-pressure recovery, 0.573; mass-flow ratio, 0.966; supercritical.

(b) Total-pressure recovery, 0.644; mass-flow ratio, 0.959; near critical.

(c) Total-pressure recovery, 0.635; mass-flow ratio, 0.903; subcritical.

Figure 7. - Profiles with no bleed at zero angle of attack. Free-stream Mach number, 3.0. Inlet II.

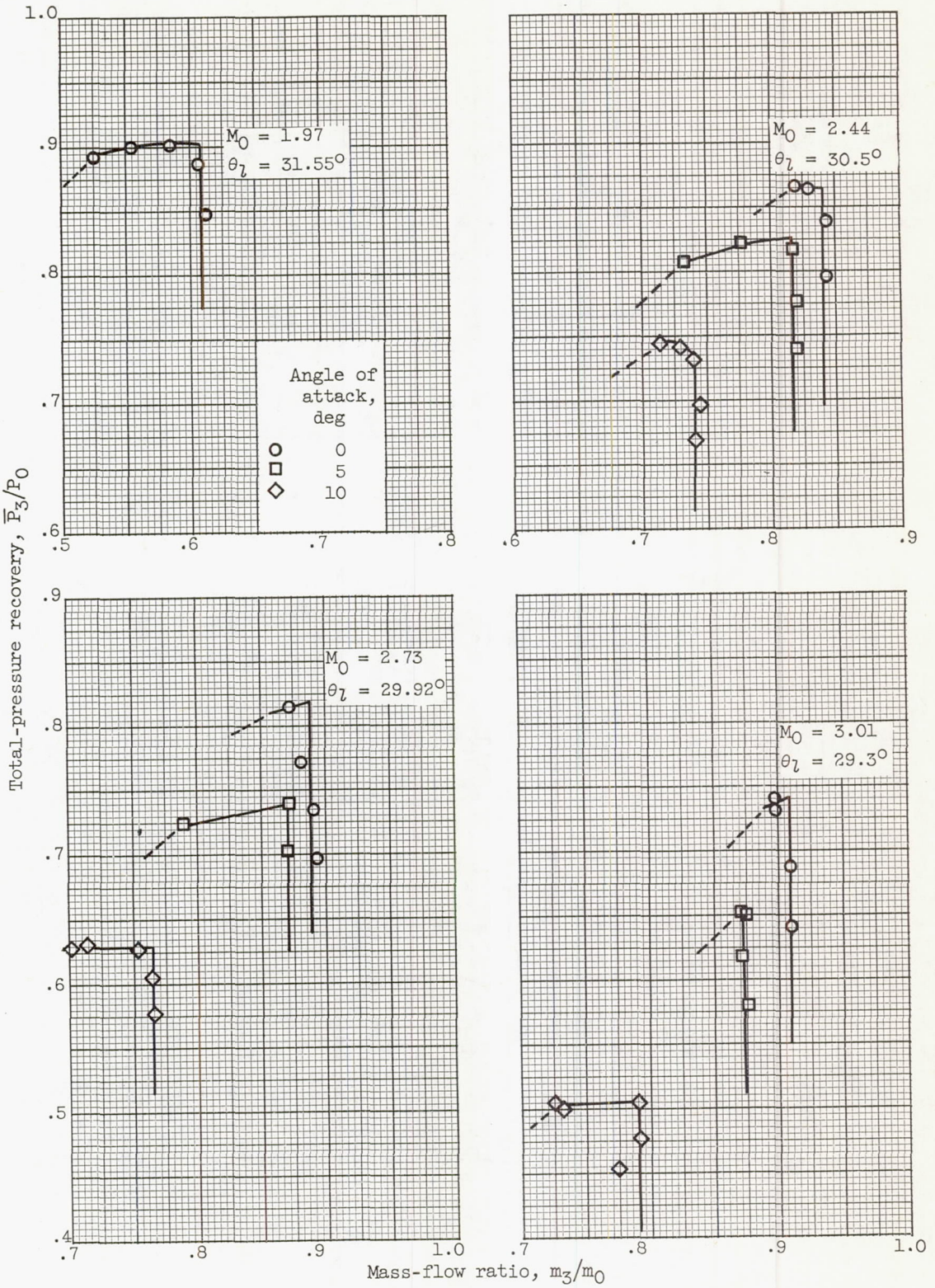

Figure 8. - Diffuser performance characteristics of inlet I with ram scoop 2.

4541

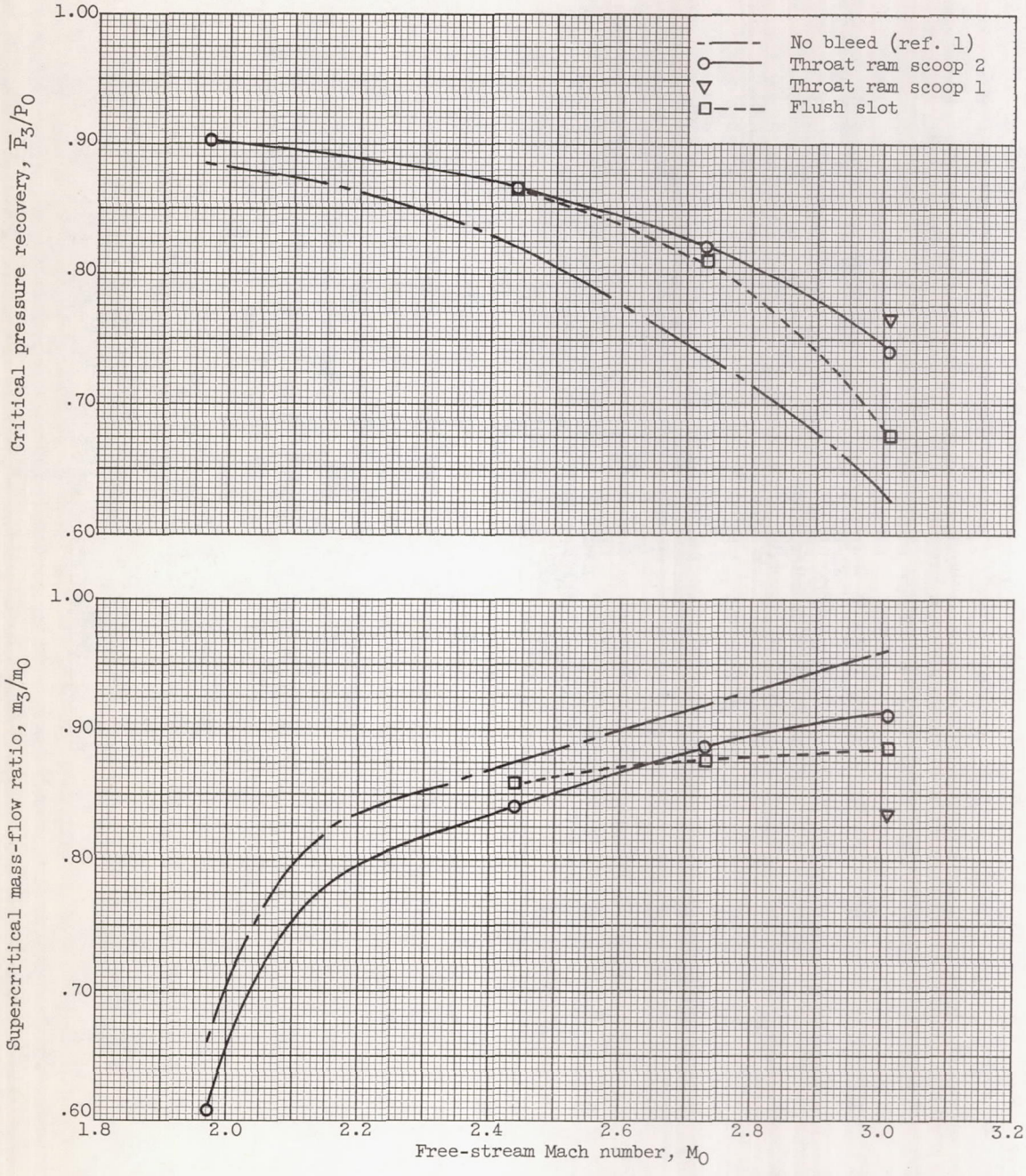

Figure 9. - Variation in critical inlet performance with Mach number. Inlet I.

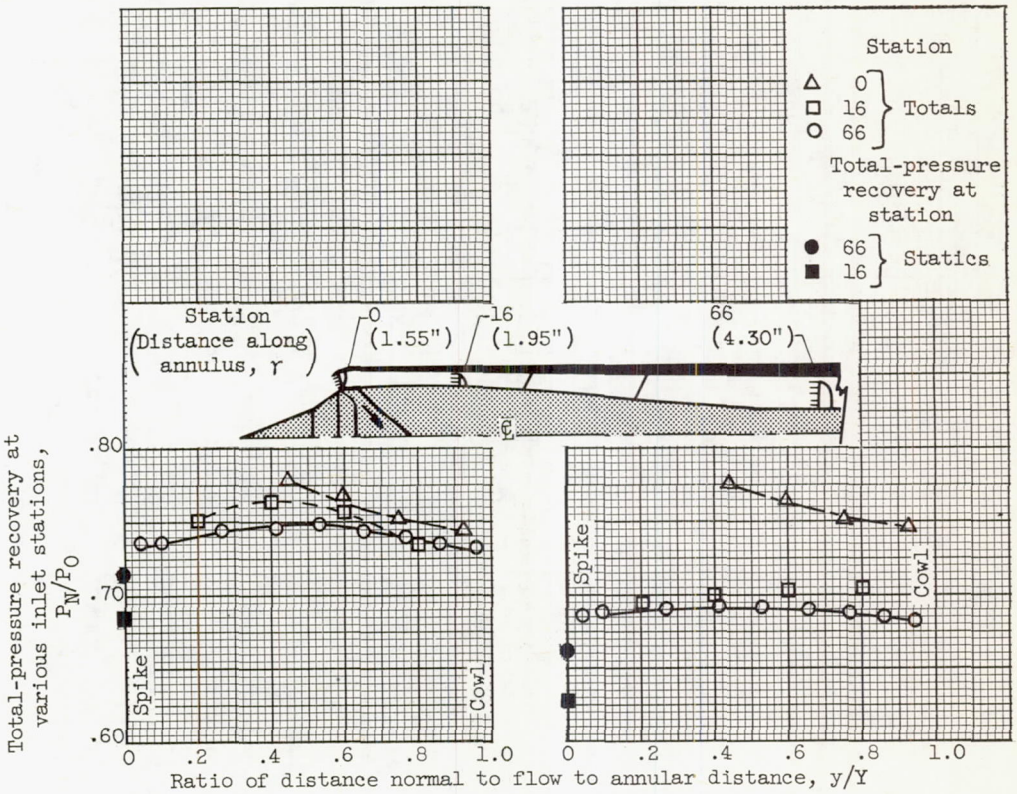

(a) Total-pressure recovery, 0.739; mass-flow ratio, 0.896; critical.

(b) Total-pressure recovery, 0.687; mass-flow ratio, 0.908; supercritical.

Figure 10. - Profiles with throat bleed at zero angle of attack (ram scoop 2). Free-stream Mach number, 3.01.

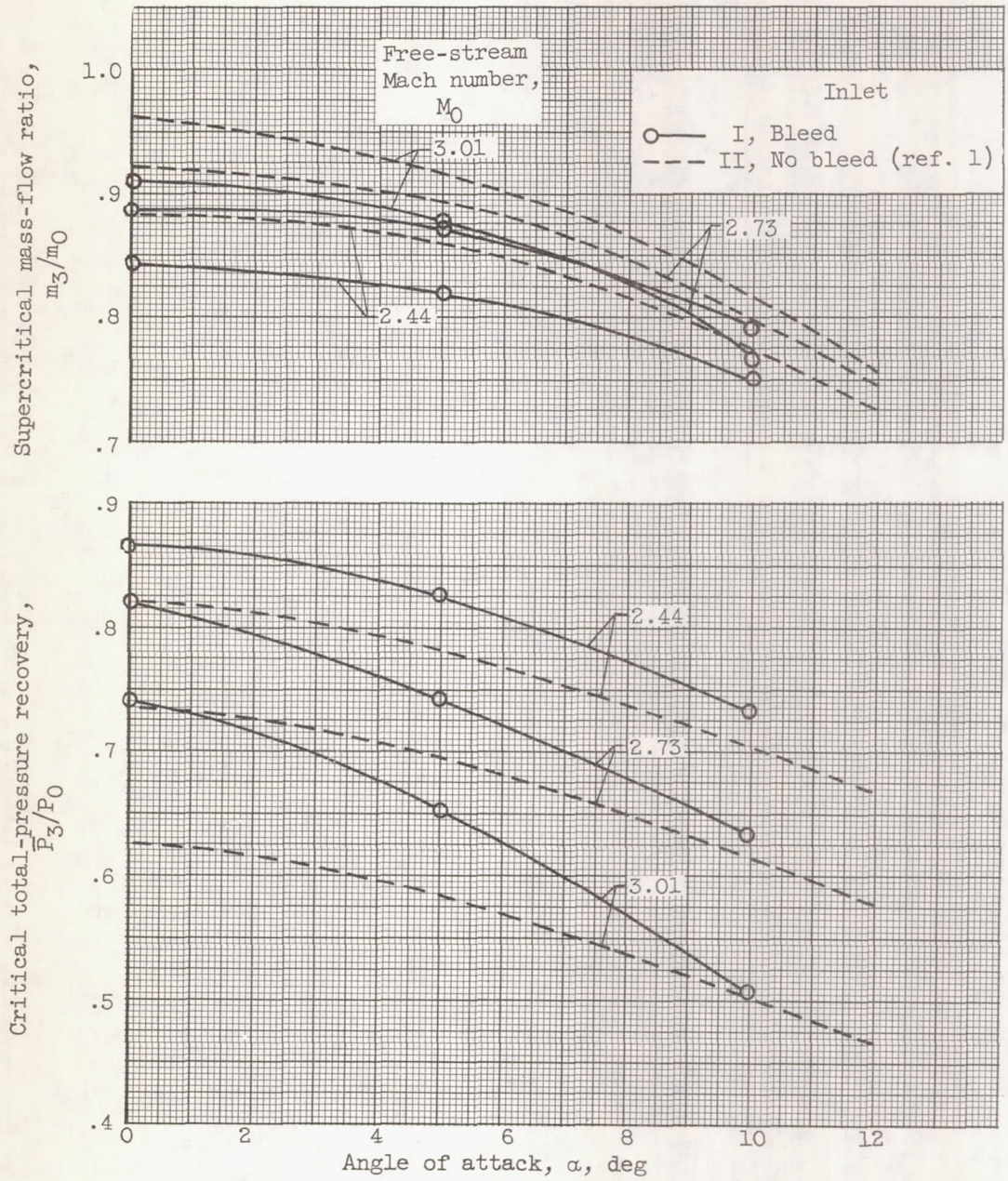

Figure 11. - Effect of angle of attack on critical inlet performance with and without boundary-layer control.

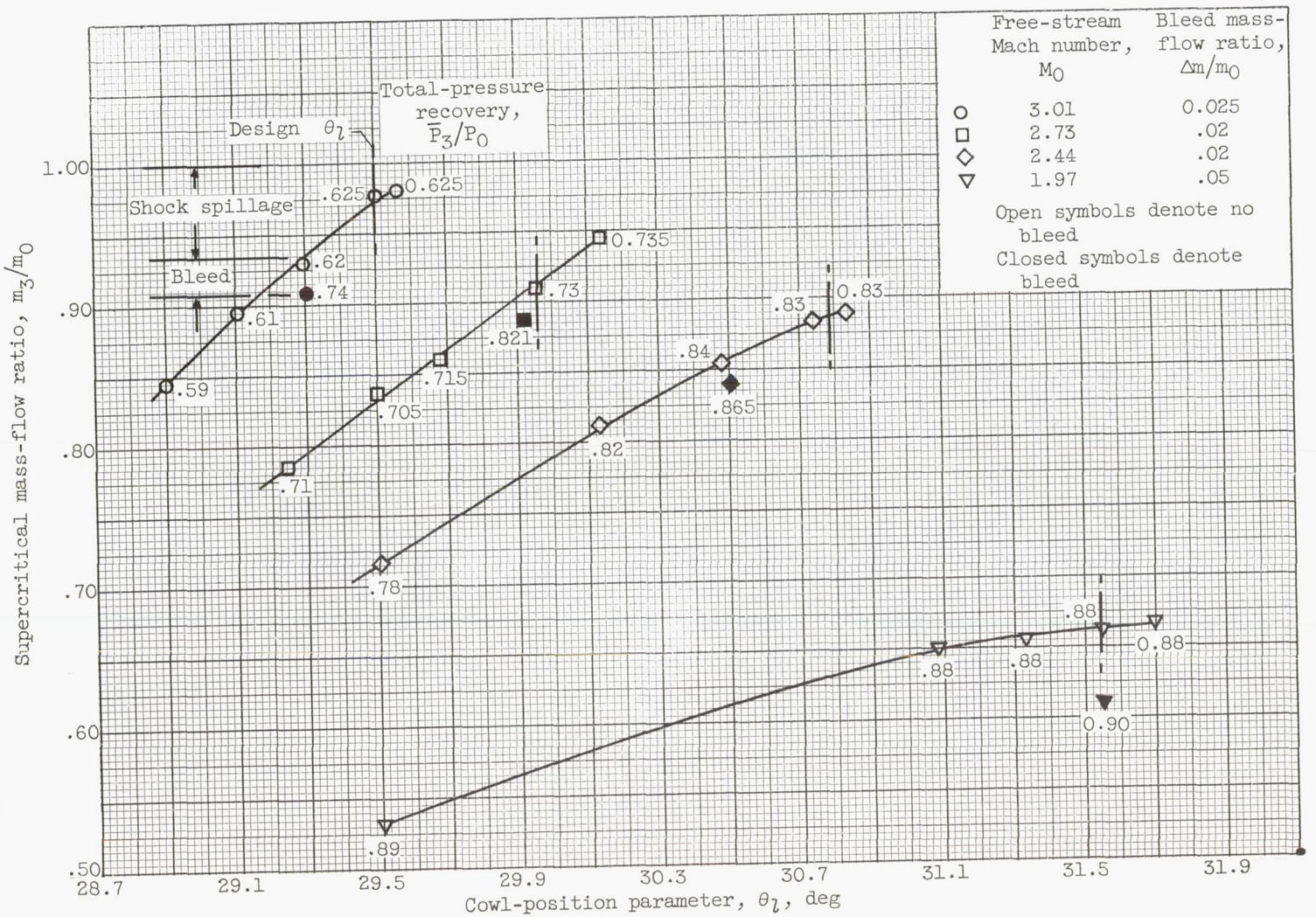

Figure 12. - Variation in mass flow and recovery with cowl-position parameter. Inlet I with and without bleed.

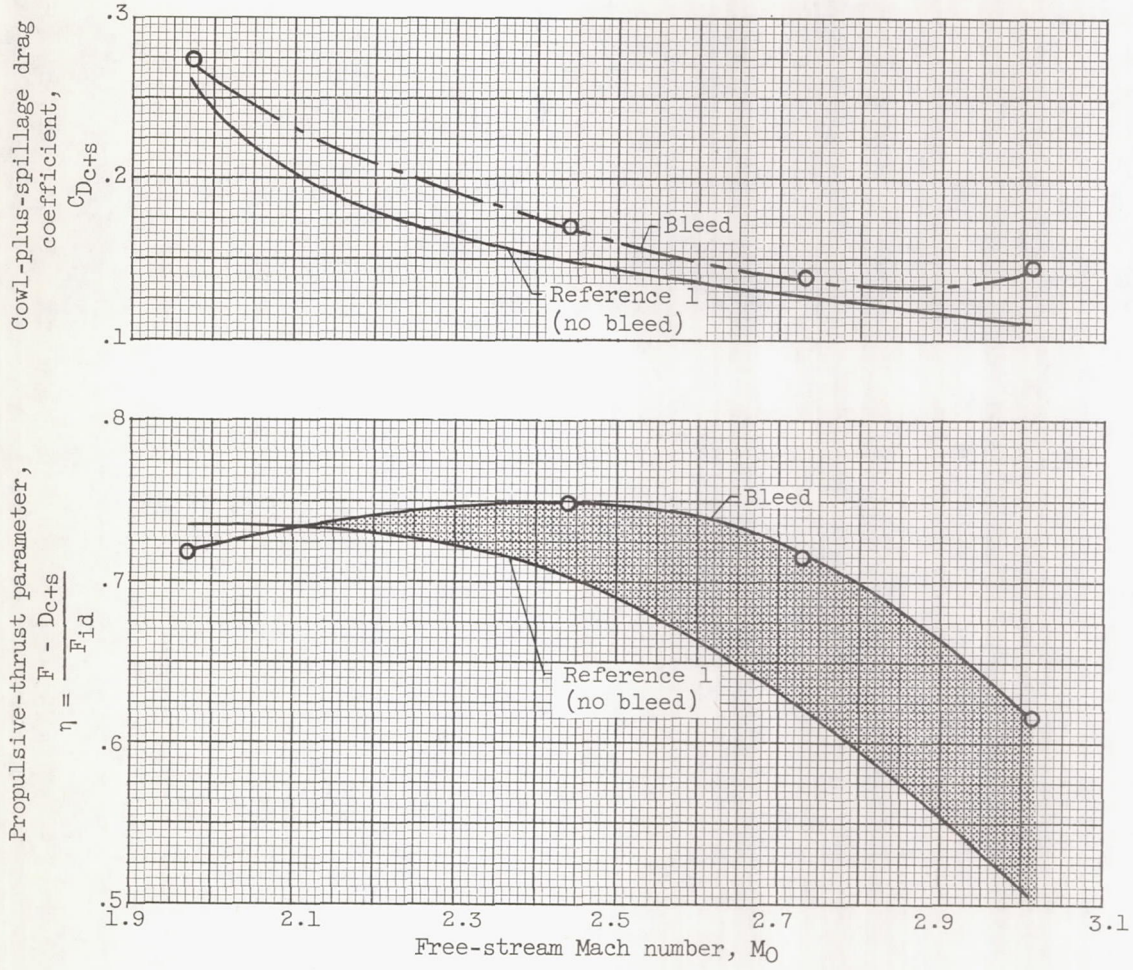

Figure 13. - Propulsive thrust comparison of translating-spike inlet I with and without throat bleed.

NOTES: (1) Reynolds number is based on the diameter of a circle with the same area as that of the capture area of the inlet.

(2) The symbol * denotes the occurrence of buzz.

Report and facility	Description			Test parameters				Test data				Performance		Remarks
	Configuration	Number of oblique shocks	Type of boundary-layer control	Free-stream Mach number	Reynolds number $\times 10^{-6}$	Angle of attack, deg	Angle of yaw, deg	Drag	Inlet-flow profile	Discharge-flow profile	Flow picture	Maximum total-pressure recovery	Mass-flow ratio	
RM E57F03 Lewis 10-by 10-ft unitary wind tunnel	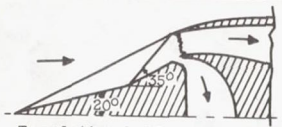 Translating double-cone axisymmetric inlet with throat ram scoop.	2	Throat ram-scoop bleed	3.01 2.73 2.44 1.97	3.07	0 to 12	0	√ √ √ √	√	√ √ √ √	√ √ √ √	0.765 .820 .865 .900	0.99 to 0.85* .95 to .78* .89 to .72* .67 to .53*	Major gains in total-pressure recovery and propulsive thrust were obtained with boundary-layer removal at the throat. Cowl projected area equal to 20 percent of A_{max}.
RM E57F03 Lewis 10-by 10-ft unitary wind tunnel	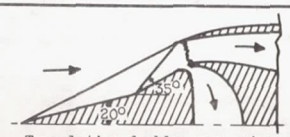 Translating double-cone axisymmetric inlet with throat ram scoop.	2	Throat ram-scoop bleed	3.01 2.73 2.44 1.97	3.07	0 to 12	0	√ √ √ √	√	√ √ √ √	√ √ √ √	0.765 .820 .865 .900	0.99 to 0.85* .95 to .78* .89 to .72* .67 to .53*	Major gains in total-pressure recovery and propulsive thrust were obtained with boundary-layer removal at the throat. Cowl projected area equal to 20 percent of A_{max}.
RM E57F03 Lewis 10-by 10-ft unitary tunnel	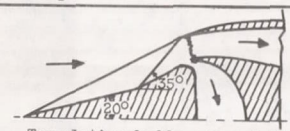 Translating double-cone axisymmetric inlet with throat ram scoop.	2	Throat ram-scoop bleed	3.01 2.73 2.44 1.97	3.07	0 to 12	0	√ √ √ √	√	√ √ √ √	√ √ √ √	0.765 .820 .865 .900	0.99 to 0.85* .95 to .78* .89 to .72* .67 to .53*	Major gains in total-pressure recovery and propulsive thrust were obtained with boundary-layer removal at the throat. Cowl projected area equal to 20 percent of A_{max}.
RM E57F03 Lewis 10-by 10-ft unitary tunnel	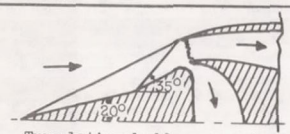 Translating double-cone axisymmetric inlet with throat ram scoop.	2	Throat ram-scoop bleed	3.01 2.73 2.44 1.97	3.07	0 to 12	0	√ √ √ √	√	√ √ √ √	√ √ √ √	0.765 .820 .865 .900	0.99 to 0.85* .95 to .78* .89 to .72* .67 to .53*	Major gains in total-pressure recovery and propulsive thrust were obtained with boundary-layer removal at the throat. Cowl projected area equal to 20 percent of A_{max}.

Bibliography

These strips are provided for the convenience of the reader and can be removed from this report to compile a bibliography of NACA inlet reports. This page is being added only to inlet reports and is on a trial basis.